Int J Fract (2025) 249:49
https://doi.org/10.1007/s10704-025-00859-x

RESEARCH

Test parameter sensitivity of the Lake-Yeoh cutting method for measurement of intrinsic strength of rubber

Nikolas Ryzí · Radek Stoček · Jakub Pawlas · William V. Mars · Thomas G. Ebbott

Received: 6 January 2025 / Accepted: 19 May 2025 / Published online: 4 July 2025

Abstract The intrinsic strength of rubber, T_0 is one of the key parameters when describing fracture behaviour of elastomer because it is at this specific value of energy that crack growth initiates within loaded rubber material. The Coesfeld Intrinsic Strength Analyzer (ISA) has been established as the most efficient equipment to directly analyse T_0 for various rubber materials. However, to obtain the most reliable and reproducible results it is crucial to understand the influence of boundary conditions of the ISA measuring methodology. Therefore, in this study sets of boundary conditions were chosen to be analysed through mechanical response of reference EPDM material with known T_0 value. For the purposes of this study the effects of individual boundary conditions were compared through directly measured value of intrinsic cutting energy, S_0 which is proportional to T_0. Blade sharpness and geometry showed the greatest impact followed by repetition of blade and specimen milling direction whereas the relaxation time and number of measuring strains showed no significant influence. The results of this study show that the knowledge of blade micro-geometry is at its most importance during the T_0 analyses. Moreover, the data clearly indicates possible future modification of boundary conditions to achieve a very efficient testing procedure with significantly reduced time required for the analyses.

Keywords Rubber · Durability · Intrinsic strength · Fatigue crack growth resistance

N. Ryzí · R. Stoček (✉) · J. Pawlas
Centre of Polymer Systems, University Institute, Tomas Bat'a University in Zlín, tř. Tomáše Bati 5678, 76001 Zlín, Czech Republic
e-mail: stocek@utb.cz

R. Stoček
PRL Polymer Research Lab, S.R.O., Nad Stráněmi 5656, 76005 Zlín, Czech Republic

W. V. Mars · T. G. Ebbott
Endurica LLC, 1219 West Main Cross Suite 201, Findlay, OH 45840, USA

1 Introduction

Rubber products are an essential part of everyday life. Due to their unique properties as is high elasticity or energy damping, they are usually used as functional element within more complex assemblies. Typical examples consist of tyres, v-belts, conveyor belts, hoses, bushings or seals and gaskets. These products are commonly used in applications where cyclic loading occurs, which causes fatigue wear and damage of the part. Additionally, many rubber components are also exposed to random, extreme loading conditions as is contact with a sharp object or edge of a metal part. All these loading conditions lead to the initiation of micro-cracks which may form not only on the surface of the components, but also in the material structure. In

both cases, the cyclic loading results in stress concentration around the tip of the micro-cracks, which can lead to their growth into macro-cracks or even to catastrophic failure. The knowledge of relation between specific tearing energy and mechanical response of a rubber material is of an enormous importance when evaluating fracture behaviour, as it can be used to efficiently optimize compound formulation to improve crack resistance as well as durability. (Li et al. 2016; Ghosh et al. 2014).

One of the most important characteristics that must be known to understand fracture behaviour of rubber is the intrinsic strength. The intrinsic strength, also referred to as T_0 is the threshold value of tearing energy required for initiating crack growth, while below this limit, the fatigue crack growth rate caused by mechanical loading is assumed to be zero. Fig. 1 (Peter et al. 2024; Lake and Lindley 1965).

There are several testing methods to characterize T_0. These include Near-Threshold Fatigue Crack Growth Analysis established by Lake and Lindley (Lake and Lindley 1965) and implemented in several studies (Stoček 2021; Zhang et al. 2018; Legorju-Jago and Bathias 2002), Tear Strength Analysis of Swollen Materials or at High Temperatures (Gent and Tobias 1982; Bhowmick et al. 1990; Mazich et al. 1991) and Cutting Method of Lake and Yeoh. (Lake and Yeoh 1978) Each of these methods have their limitations from high measuring time demands to mere estimation of T_0. Nevertheless, the Cutting Method of Lake and Yeoh has emerged as the most promising one and has been implemented in in-situ measuring device the Intrinsic Strength Analyser (ISA) developed by COESFELD GmbH & Co. KG (Germany) (Fig. 2) with implemented testing protocol developed by Endurica LLC (OH, USA).

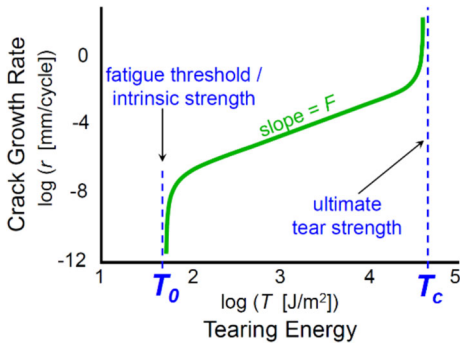

Fig. 1 Fatigue crack growth rate curve (Peter et al. 2024)

Fig. 2 Intrinsic Strength Analyser

However, this method is nowadays already applied so for the analysis of intrinsic strength, T_0, outside of rubber materials invariably for the analysis of casting polyurethane (CPU). CPU is a crucial material in various sectors, such as construction, healthcare, and the automotive industry (Jin et al. 2025). Thus, it is evident that this method is becoming established in various sectors, and it is necessary to detail this method so that it is clearly reproducible across a spectrum of different materials.

This study aims to extend already well-established ISA measuring methodology by performing a comprehensive analysis of the effect of various boundary conditions on the T_0 measurement, using reference material, which has extensively been studied by Near-Threshold Fatigue Crack Growth Analysis to obtain an exact T_0 value. More details can be found in the previous publication of the authors (Stoček 2021).

Considering that the ISA device is the only equipment specifically developed to analyse the value of intrinsic strength T_0, both for science and industry, it is highly appropriate to demonstrate the influence of the test protocol variations on the accuracy of T_0 measurement. And it is precisely this question that our study focuses on in detail. The results aim to create a clear overview of the effects of individual parameters of the testing protocol on the T_0 measurement so that this methodology becomes maximally efficient and accurate.

In the past studies fundamental work was carried out and some of the conditions and their effects on rubber behaviour near T_0 has already been discussed. These mainly include investigations of rubber formulation effects as in (Robertson et al. 2019; Robertson et al. 2019) where the influence of polymer type on T_0 were investigated, the influence of reinforcing fillers

(Robertson et al. 2019; Isitman et al. 2020) or the crosslinking effect. (Robertson et al. 2019; Isitman et al. 2020) Furthermore the influence of aging effect of temperature on T_0 of rubber vulcanizates was described in. (Robertson et al. 2019).

And finally, the influence of some of the measuring conditions in ISA methodology on resulting T_0 were studied, namely velocity of the cutting blade and specimen pre-force (Stoček et al. 2017, 2015), geometry of crack tip (Lake and Yeoh 1987) and specimen thickness and blade sharpness. (Mars et al. 2022).

Based on the previous findings this study will focus on addressing additional measuring conditions which could potentially be responsible for affecting the reliability and accuracy of the measurement. The main goal is to subsequently decrease possible negative effects of these conditions on the precision of the ISA measuring methodology and thus improve it. Chosen conditions in focus consist of cutting blades' geometry and sharpness, material's relaxation time and its polymer chain orientation and number of applied measuring strains. These conditions have not been investigated prior to this work or a detailed verification of their effects is needed. Resulting effects of the individual conditions will be compared through intrinsic cutting energy S_0 (Eq. 3) using reference EPDM material (Table 5) with known intrinsic strength $T_0 \approx 50$ J/m^2, which has been determined using Near-Threshold Fatigue Crack Growth analysis. (Stoček 2021) Using intrinsic cutting energy, S_0 as the final comparison tool ensures profound description of the effects of the conditions on the measurement it-self while retaining relation to the reference material.

2 Experiment and materials

The measurement principle shown in (Fig. 3) is based on a standard ISA testing methodology presented in (Fig. 4) consists of several steps and was thoroughly described in Robertson et al. (2021). First, each test specimen is preconditioned using maximal measuring strain. Then an initial cut is performed ensuring the position of the crack tip in the plane strain (PS) region of the sample as is discussed in Stoček et al. (2013); Stoček et al. 2020; Eberlein et al. 2020). Initial cut is followed by a series of deformations using progressively increasing measuring strains accompanied by relaxation phase to account for viscous behaviour of rubber. And finally, after each relaxation phase a cutting sequence composed of three individual cutting rates begins. First cutting rate is applied to establish a well-defined crack path. Second stabilizes the crack path and third, the lowest rate, minimizes the hysteresis at the crack tip so any remaining energy can be associated only with breaking of polymer chains.

Through the analysis, stretching force, f_s, cutting force, f_c and displacement of sample and cutting blade are being recorded. Data evaluation to obtain the intrinsic cutting energy, S_0 and subsequent intrinsic strength, T_0 consists of determining tearing energy, T and cutting energy, F.

For an edge cracked planar test specimen (PS), also known as pure-shear sample (Fig. 3) the tearing energy, T is dependent on the strain energy density, W obtained by integration of strain function derived from stress—strain curve and undeformed sample length, L_0:

$$T = W \bullet L_0 \tag{1}$$

Cutting energy, F is the ratio of cutting force, f_c and specimen thickness, t:

$$F = \frac{f_c}{t} \tag{2}$$

The sum of the tearing energy, T and cutting energy, F then equals to intrinsic cutting energy, S_0:

$$S_0 = T + F \tag{3}$$

Which can be used to determine intrinsic strength, T_0:

$$T_0 = S_0 \bullet b \tag{4}$$

where b is a constant relevant to the blade's geometry. (Robertson et al. 2019, 2021; Mars et al. 2022).

2.1 Boundary conditions

To analyse reference S_0 value a default testing protocol listed in Table 1 was used. Subsequently a full study of effects of individual variation of boundary conditions:

a) number of measuring strains,
b) duration of relaxation time,
c) repetition of blade,
d) orientation of the polymer chains,
e) geometry of the blade, were conducted.

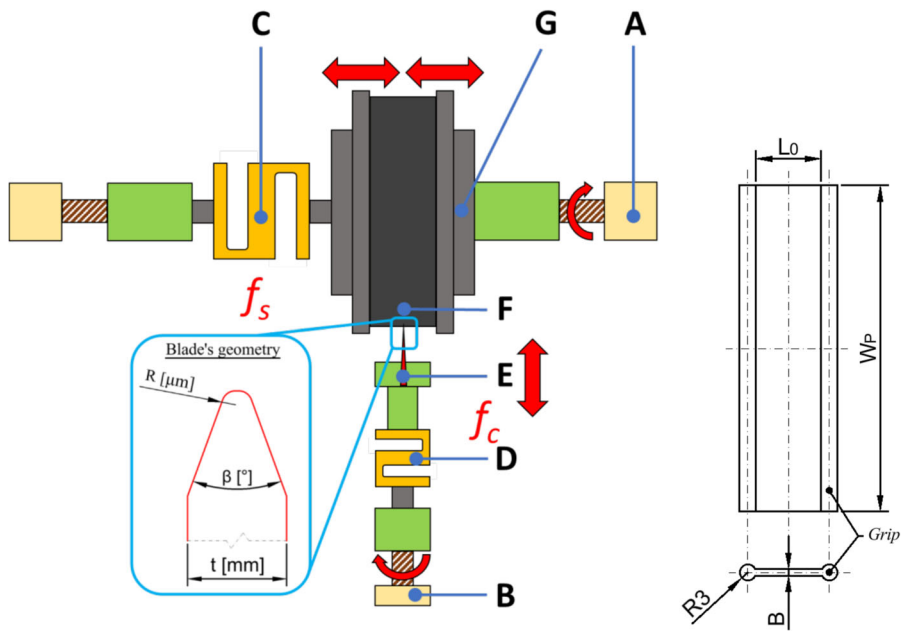

Fig. 3 A schematic of the ISA measuring principle (left), with: stretching actuator **A**; cutting actuator **B**; stretching load cell **C**; cutting load cell **D**; razor blade **E**; sample **F**; clamping system **G**; Pure-shear specimen geometry (Right)

a) To analyse the effect of the number of measuring strains ε_N five sub—conditions were evaluated as listed in Table 2. For each sub—condition the lowest strain value ε_{min} was 1% and the highest ε_{max} 12% of L_0.

b) To analyse the effect of relaxation time, five measurements were conducted using relaxation time of 6 s, 60 s, 180 s, 300 s and 600 s.

c) The analysis of blade repetition, in other words repeated use of the identical spot of the blade, was carried out using 3 different type of blades, whereas all applied blades had a thickness of 0.1 mm. The list of applied blades and their detailed description is given in Table 3. This part of the study focuses on the analysis of blade blunting and its influence on the measured parameters. Therefore, razor blades with different blade surface treatment were selected and compared with uncoated blades. It was assumed that the surface treatment should ensure the stability of the blade without dulling it. Therefore, each single blade at the identical spot was applied for six separate measurements.

d) Together with the analysis of blade repetition an analysis of the effect of specimen milling direction was carried out. Two series were performed with the milling direction perpendicular to the cutting direction and parallel to the cutting direction as described in Fig. 5. Prior to vulcanization, rubber compound was prepared on a double-roll mill, which induces strong shearing flows in the uncured rubber, and therefore the potential for a preferred orientation of polymer chains.

e) The analysis of blade's tip geometry effect was carried out using seven different blades with various defining thicknesses ranging from 0.1 mm to 0.68 mm. Furthermore, a scanning electron microscope (SEM); TESCAN VEGA 3, Tescan, Czech Republic; was used to evaluate micro-geometry of blades' tips thus obtaining detailed tip radius R and tip angle β values for individual blades. (Table 4)

Only one boundary condition was changed for each performed analysis, others were left unchanged according to default testing protocol. Analyses were performed at 25 °C and three repetitions were performed for each measurement.

Additionally, a FEM analysis using blades' geometries obtained by SEM was carried out to gain an insight on which specific dimension of the blade has the fundamental impact onto its' effect. The analysis

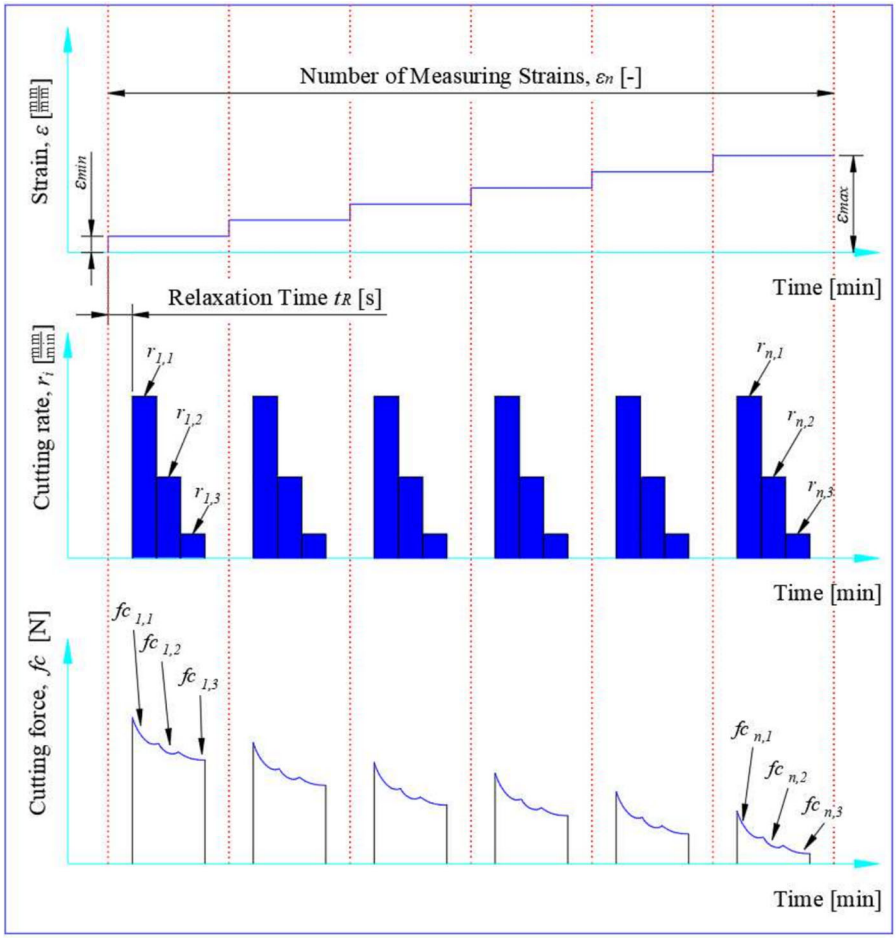

Fig. 4 ISA standard testing methodology scheme

Table 1 ISA default testing protocol

Boundary condition	Value
Preconditioning speed	0.6 mm/L_0/min
Preconditioning maximal strain	50%
No. Precondition cycles	5
Depth of initial cut	18 mm
Relaxation time, t_R	10 min
Cutting rates of blade, r_i	10, 0.1, 0.01 mm/min
Displacements of the blade	4, 0.4, 0.04 mm
Number of measuring strains, ε_N	10
Strain values	1, 2, 3, 4, 5, 6, 7, 9, 10, 12% of L_0
Blade thickness, t	0.1 mm

was designed and evaluated using ABAQUS CAE 2016 according to conditions and parameters listed in Table 5 and assembly visualization in Fig. 6.

2.2 Material

Within the framework of this study ethylene-propylene-diene rubber (EPDM) type Keltan® 4465

Table 2 List of strain range densities used in the study

Number of measuring strains, ε_N	Strain values, % of L_0
3	1, 5, 12
5	1, 2, 5, 8, 12
7	1, 2, 3, 4, 8, 10, 12
9	1, 1, 2, 4, 5, 6, 8, 10, 12
11	1, 1, 2, 3, 4, 5, 6, 7, 9, 10, 12

Table 3 List of blades used for study of blade repetition influence

Blade thickness t, mm	Producer	Blade surface treatment	Specification	Customs code
0.1	Lutz Blades Solingen/Germany	no treatment	0410.0100	S00673-0
0.1	Lutz Blades Solingen/Germany	Titan-Nickel	0410.0100/TiN	S01648
0.1	FortisBlades Zwevegem/Belgium	Ceramic	20.80.082.010	82089000

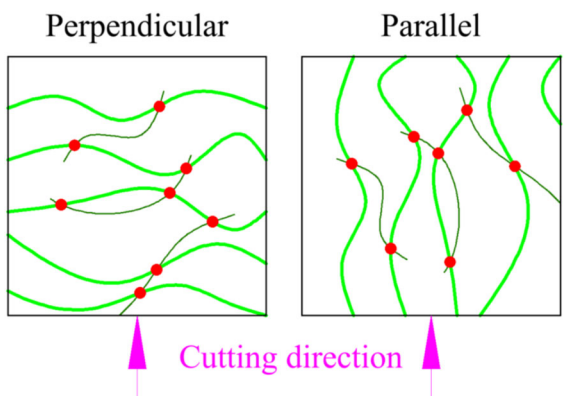

Fig. 5 Definition of polymer chains' orientation towards cutting direction

(ARLANXEO, Netherlands B.V.) was chosen as a reference material. The compound was filled with 70 phr (parts per hundred of rubber) of carbon black (CB) type N550 and crosslinked with a sulphur-based curing system. The complete formulation is listed in Table 6. The glass transition temperature of the subject material was − 50 °C, whereas the value has been determined using dynamic mechanical analyses (DMA) performed with DMA Analyser TMA/SDTA 841 (Mettler Toledo, Switzerland).

Rubber compound was prepared in a two-step mixing procedure, where both steps were carried out using an internal mixer SYD-2L (Everplast, Taiwan) of 1.5 L capacity and with a fill factor of 0.7. In the first step rubber and reinforcing fillers were mixed for 4 min with rotor speed set to 50 rpm and temperature to 150 °C. In the second step, the curing system and the rest of the compound components were added and mixed for 3 min at 35 rpm and temperature of 110 °C thus completing the final batch. After mixing, the compound was milled and sheeted using a two-roll mill at a rolling temperature of 60 °C and subsequently stored for 24 h before curing.

Curing properties were determined using a moving die rheometer MDR 3000 Basic (MonTech, Germany), according to ASTM 6204 and the optimum cure time, t_{90}, was found to be 7.16 min.

The pure-shear test specimens were cured using a compression mould in a heat press LabEcon 300 (Fontijne Presses, Netherlands) at the temperature of 175 °C and with respect to the optimal curing time t_{90}. The geometry of the used test specimens is shown in Fig. 3. The geometrical dimensions were as follows: length L_0 = 10 mm, width W_p = 100 mm, radius of gripping collars R = 3 mm and thickness B = 1.5 mm.

3 Results and discussion

This part of the study provides and discuss obtained results of the effects of various ISA measuring

Table 4 List of blades used in the study

Blade thickness, t [mm]	Tip radius, R [μm]	Tip angle, β [°]	Product number
0.1	0.46	57	S00673-0
0.13	1.2	46	S00505-0
0.15	1.04	53	S00494-0
0.2	1.08	51	S00486-0
0.3	0.94	53	S00484-0
0.4	1.24	55	S01262-0
0.68	1.78	47	S14529-0

Table 5 List of parameters for FEM analysis

Parameter	Value
Analysis type	Static, General
Analysis method	Frictionless contact method
Sample model type	2D, Deformable Plane
EPDM Hyper-elastic model	Yeoh; C10 = 1.3, C20 = − 0.7, C30 = 0.3
Sample element type	3-node linear plane stress triangle, CPS3
Sample element size	0.1 μm
Blade model type	2D, Rigid Wire
Blade element type	2-node 2-D linear rigid link, R2D2
Blade element size	0.08 μm
Loading—Displacement, U	0.015 mm
Resulting Data	Reaction force, F_R [N]; Max. Von Mises, Stress, σ [MPa]

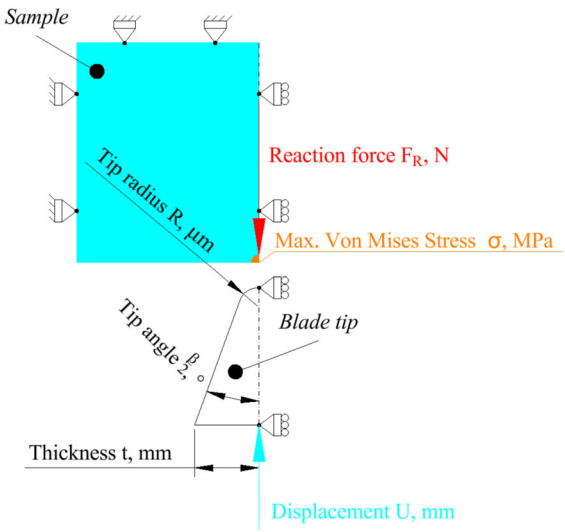

Fig. 6 FEM analysis assembly visualization

boundary conditions on to the resulting intrinsic cutting energy, S_0. Furthermore, a relation between geometrical properties of used blades and the resulting intrinsic cutting energy S_0 has been investigated through SEM images and FEM analysis.

Fig. 7 A shows the effects of the number of applied measuring strains on intrinsic cutting energy S_0 according to conditions listed in Table 2. The resulting linear trend shows slight decrease in S_0 with increasing number of measuring strains. However, considering the standard deviation for individual S_0 values the overall decreasing trend is not considered significant. This suggests that the testing protocol can be shortened by using lower number of measuring strains, thus decreasing overall duration of the analysis

Fig. 7 B shows the effect of the duration of relaxation time on intrinsic cutting energy S_0. The resulting linear trend shows slight increase in S_0 with increasing relaxation time. However, as in the previous case, if we consider individual values together with their standard deviations the increasing trend is not consider significant. This points out to the assumption that the preconditioning phase and its parameters introduced in Table 1 are sufficient to counter the viscous behaviour of rubber. However, it must be noted that this study focuses only on one

Table 6 Rubber compound recipe

Production step	Component	Chemical denotation	Type	Content, phr
Master Batch	Rubber	Ethylene-propylene-diene rubber	EPDM	100
	Filler	Carbon black	N550	70
Final Batch	Antiozonant	N-(1,3- Dimethylbutyl)-N′- phenyl-p-phenylenediamine	6PPD	1.5
	Activator	Zinc oxide	ZnO	3
	Activator	Ostadecanoic acid	Stearic acid	1
	Accelerator	N-Cyclohexyl-2-benzothiazole Sulfenamide	CBS	3.2
	Cross-linking agent	Sulphur	S	1.7

reference EPDM material. Different behaviour might apply for different rubber types as their viscous properties as is relaxation time varies. (Tobolsky et al. 1944) This concerns not only type of rubber but the whole rubber compound, as for example different CB loading influence viscous behaviour as well. (Mostafa et al. 2009)

Fig. 7 C firstly shows the effect of blade repetition on intrinsic cutting energy S_0 for the standard blade with untreated surface. The resulting trends show high increase in S_0 with each additional blade re-use up to the maximal number of investigated repetitions. These results correspond with previous study (Mars et al. 2022) where effects of blade sharpness on S_0 were also

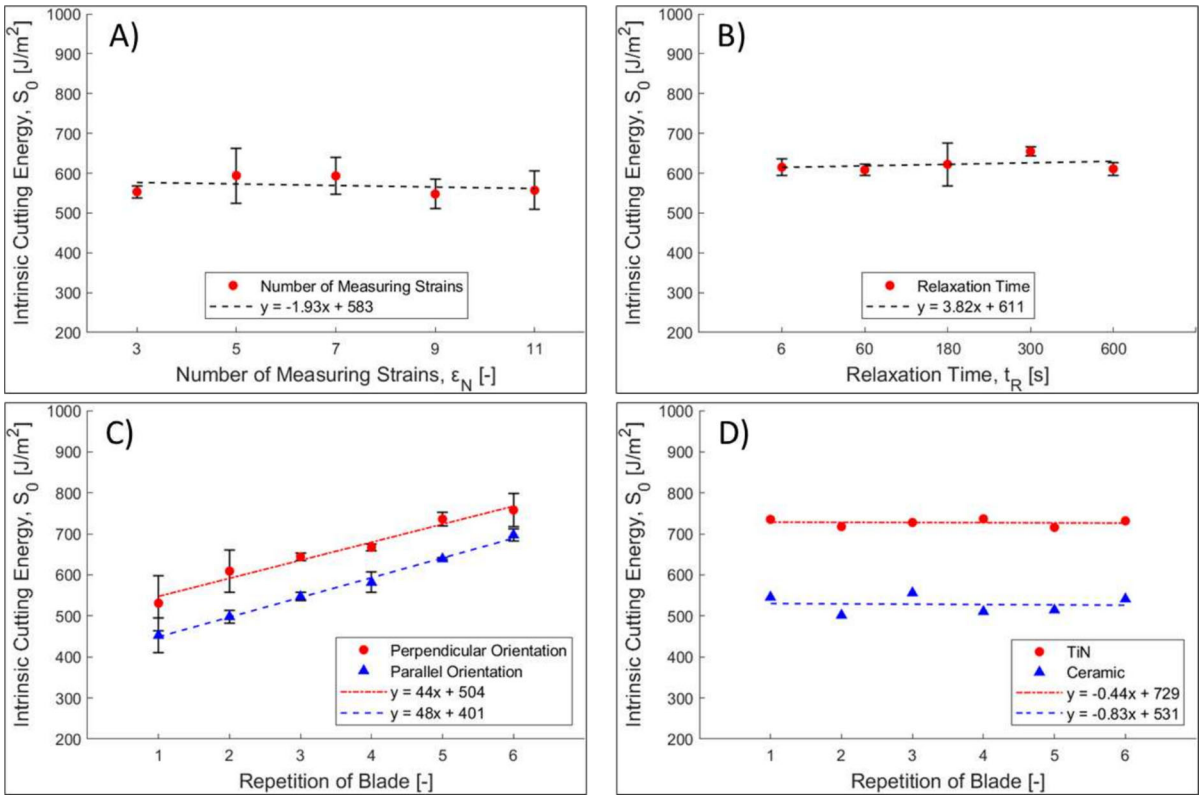

Fig. 7 **A** Effect of applied strain range density on intrinsic cutting energy; **B** Effect of relaxation time on intrinsic cutting energy; **C** Effects of sample orientation and blade repetition on intrinsic cutting energy for untreated blade; **D** Effect of blade repetition on intrinsic cutting energy for coated razor blades

investigated. However, in comparison with previous findings these results show more linear than exponential increase in S_0. This could potentially make detecting an error in blade re-use more difficult. Furthermore, figure shows a significant offset in S_0 when it comes to polymer chains' orientation. Perpendicular orientation of polymer chains towards cutting direction has shown higher S_0 values than parallel orientation. This suggest that if the polymer chains are oriented perpendicularly towards cutting direction the blade has to overcome higher material resistance by increasing cutting force. This confirms that the knowledge of polymer chains' orientation is at outmost importance for the consistency and precision of measurements

In Fig. 7D, on the other hand, the intrinsic cutting energy, S_0 values using treated blades for 6 repetitions of the same blade location on each razor blade are shown. Both surface treatments provide the ability to protect the blade so that it does not dull and identical values of intrinsic cutting energy, S_0, can be analysed independent on the number of repetitions. All samples analysed, were measured in the perpendicular direction. The ceramic coating ensured stable and identical S_0 values that were measured when the uncoated razor blade was firstly used. Conversely, the TiN blade coating, while also causing stable values independent of the number of times the same blade site was used, significantly increased the S_0 value. These increased values may be due to either the higher friction coefficient of the TiN treatment or the higher thickness of the TiN surface layer compared to the ceramic layer. These two parameters have a direct influence on the measured cutting force and the resulting S_0 value.

Fig. 8A and B show the effects of blades' geometrical parameters on intrinsic cutting energy, S_0. The first look on the data suggests that the thickness of the blade is the leading influence as thicker the blade is the higher increase in S_0 can be observed. However, more detailed look indicates that rather than the thickness of the blade the micro-geometries are of the main influence. More specifically, the data trend of tip radius R (Fig. 8A) highly corelates with the trend of S_0 where the larger tip radius is the higher S_0 was evaluated whereas tip angle β shows opposite trend. This is confirmed by Fig. 8C where the data are fitted with a linear function showing highly increasing trend in S_0 with increasing tip radius and decreasing S_0 with increasing tip angle. These findings are in great agreement with previous works (McCarthy et al. 2007, 2010) where tip radius was found to be the most influential variable when it comes to the blade's sharpness. The smaller the investigated tip radius was the sharper the blade, resulting in decrease in cutting force therefore decrease in intrinsic cutting energy S_0

Furthermore, the results of the influence of blades' micro-geometry are supported by SEM photographs showed in Fig. 9. The figure shows three individual blades, and the measuring method used to obtain values of their micro-geometries. Additionally, on Fig. 9C a SEM photograph of used 0.13 mm thick blade can be seen. This photograph was taken after the measuring cycle and describes dulling mechanism. The blade's tip is highly deformed, visually increasing its tip radius. Therefore, it can be assumed that in the analysis of blade's repetition (Fig. 7C) the same dulling mechanism was present gradually deforming the blade's tip and thus increasing its radius and subsequently obtained S_0.

Table 7 shows overall comparison of the effects of the measuring boundary conditions through curve slope value m obtained from the individual linear fits. Although the values of slopes, m for the individual dependencies are expressed quantitatively, their comparison can only be considered qualitatively due to the different physical significance of the individual dependencies. Thus, the comparison only expresses the qualitative significance of the influence of the individual methods from most to least influential and cannot be compared and interpreted more physically with each other.Repetition of uncoated blade44 (perpendicular) / 48 (parallel)Blade's angle, β− 15.1Relaxation time, tR3.82Number of measuring strains, εN− 1.93Repetition of ceramic coated blade0.83Repetition of TiN coated blade− 0.44
Blade's radius R was evaluated as the most influential parameter with the highest effect on resulting value S_0. Repetition of uncoated blade showed the second highest effect followed by blade's angle β. In comparison with the first three conditions and parameters the effect of relaxation time as well as number of measuring strains can be considered negligible. Repeated use of the coated razor blade was found to have no effect on the change in S_0 value, with the S_0 values measured with the ceramic-treated razor blade being identical to the first S_0 value measured on the uncoated razor blade. However, reuse of the TiN-coated razor blade, although measuring constant S_0

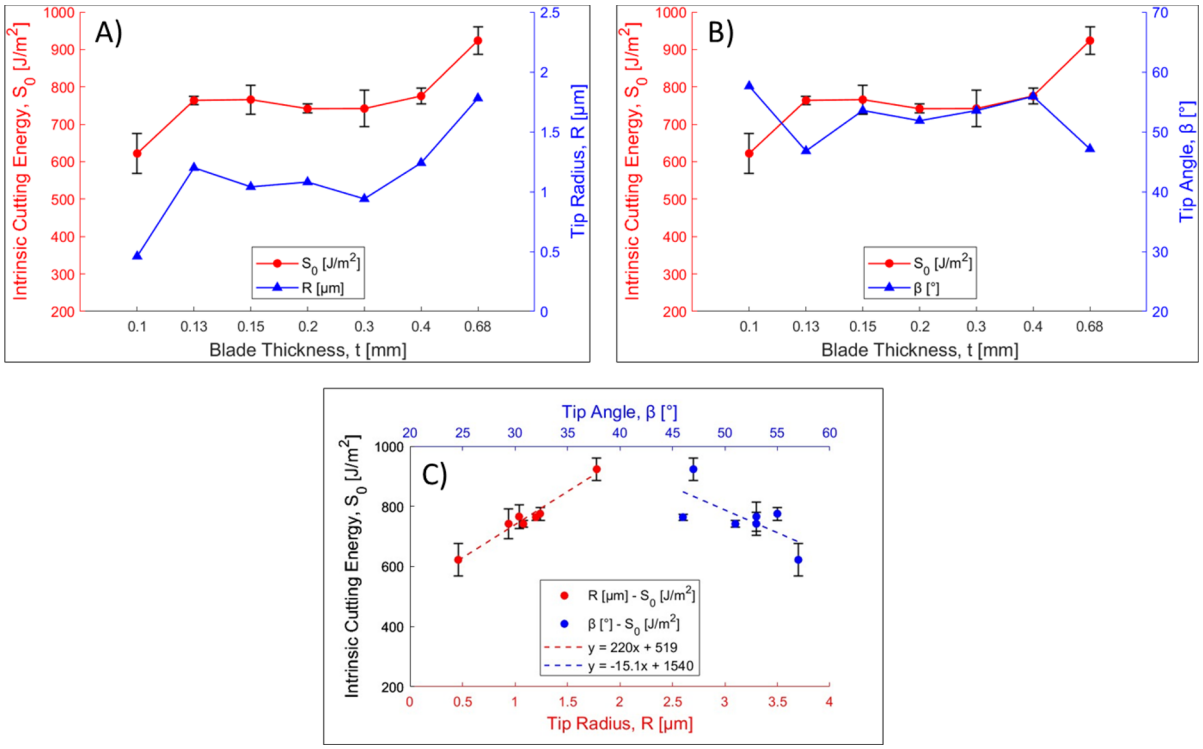

Fig. 8 **A** Effect of tip radius R on intrinsic cutting energy; **B** Effect of tip angle β on intrinsic cutting energy; **C** Linear dependence of tip radius R and tip angle β on intrinsic cutting energy

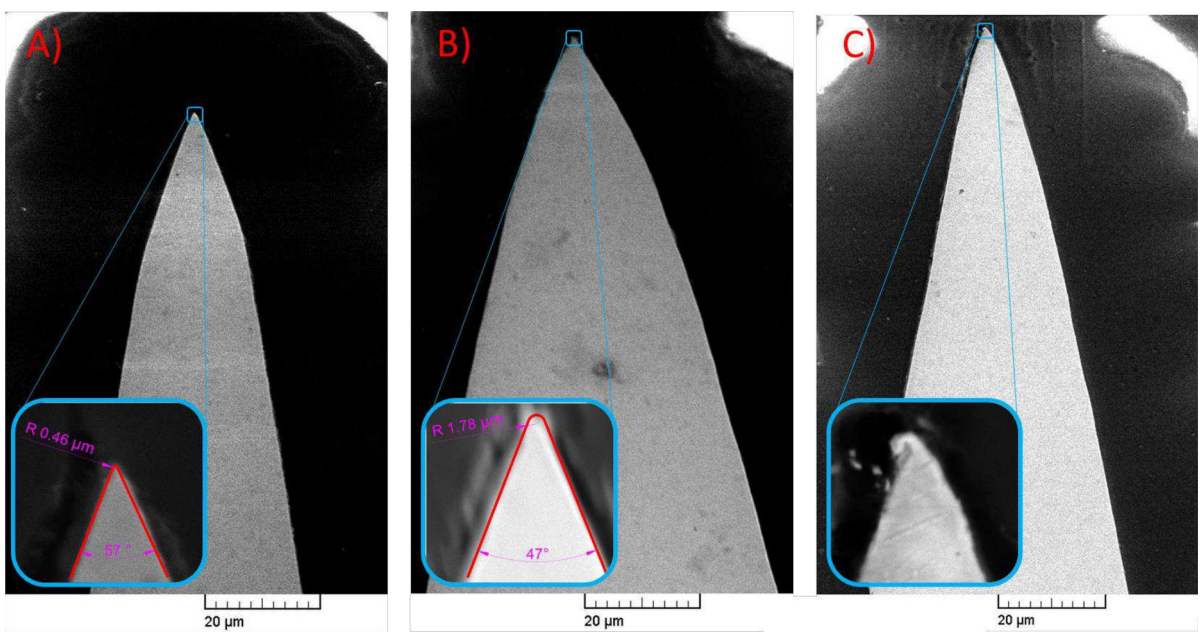

Fig. 9 SEM photographs of blades' tips according to their thickness: **A** 0.1 mm; **B** 0.68 mm; **C** 0.13 mm—USED

Table 7 Comparison of the influence of the individual boundary conditions

Boundary condition and parameters	Slope, m [-]	Influence of parameters from highest to lowest
Blade's radius, R	220	
Repetition of uncoated blade	44 (perpendicular) / 48 (parallel)	
Blade's angle, β	-15.1	
Relaxation time, t_R	3.82	
Number of measuring strains, ε_N	-1.93	
Repetition of ceramic coated blade	-0.83	
Repetition of TiN coated blade	-0.44	

values, is significantly higher than the first value measured on the uncoated razor blade.

3.1 FEM

Figures 10 and 11 show results of the FEM analysis. The data follows expected correlating trends with previous findings (Mars et al. 2019) namely increasing reaction force F_R with increasing value of tip radius R as well as increasing maximal Von Mises stress σ with decreasing value of tip radius R. Additionally, the data shows a highly correlating trend between tip angle β and maximal Von Mises stress σ. This indicates interlinked dependence of both tip radius and tip angle and their mutual geometrical effect on the practical measurement of intrinsic cutting energy S_0.

With demonstrated corelation between practical measurement and data obtained through FEM analysis a systematic FEM analysis of the influence of tip radius R and tip angle β could have been carried out. Figure 12 shows results of the systematic FEM analysis. Circles represent data where tip radius R was varied from 0.4 µm up to 30 µm. Triangles represent data where tip angle β was varied from 35° up to 130°. Red colour represents the results for reaction force F_R whereas blue colour for maximal Von Mises stress, σ, which here expresses the stress associated primarily with crack growth during cutting with a sharp razor blade.When increasing the size of tip radius, the reaction force increases linearly while maximal Von Mises stress decreases following the power law. In comparison when increasing the blade angle, the reaction force increases following

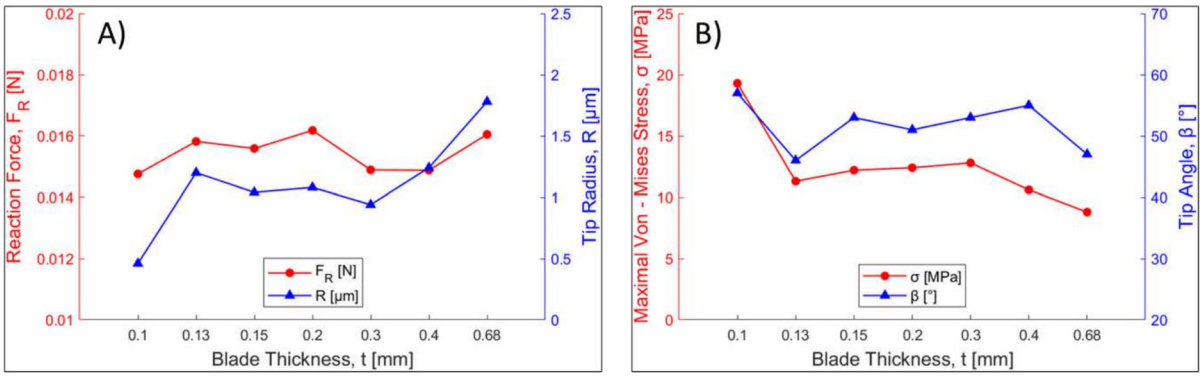

Fig. 10 FEM analysis: **A** Effect of tip radius R on reaction force F_R; **B** Effect of tip angle β on maximal Von Mises Stress σ

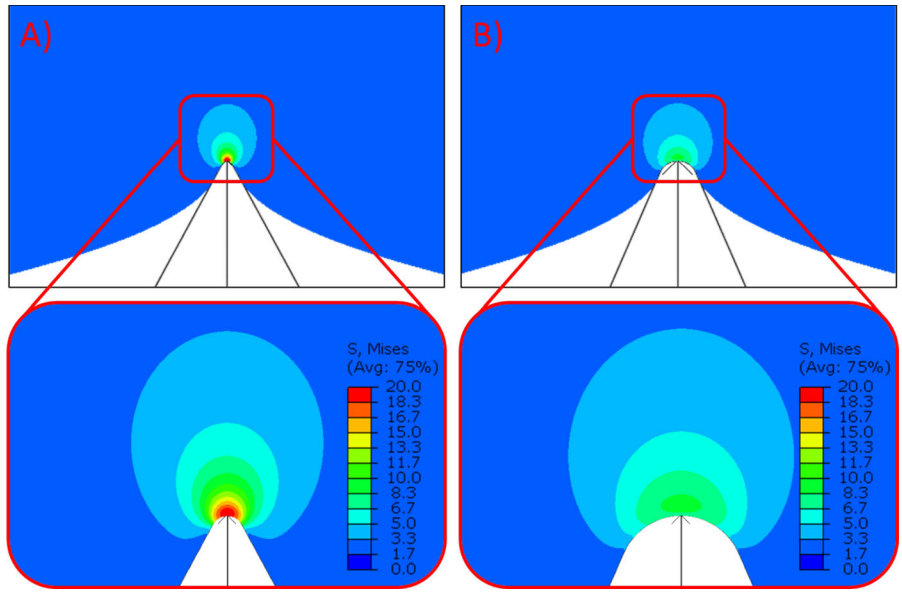

Fig. 11 Graphical visualization of FEM maximal Von Mises Stress σ according to blade thickness: **A** 0.1 mm; **B** 0.68 mm

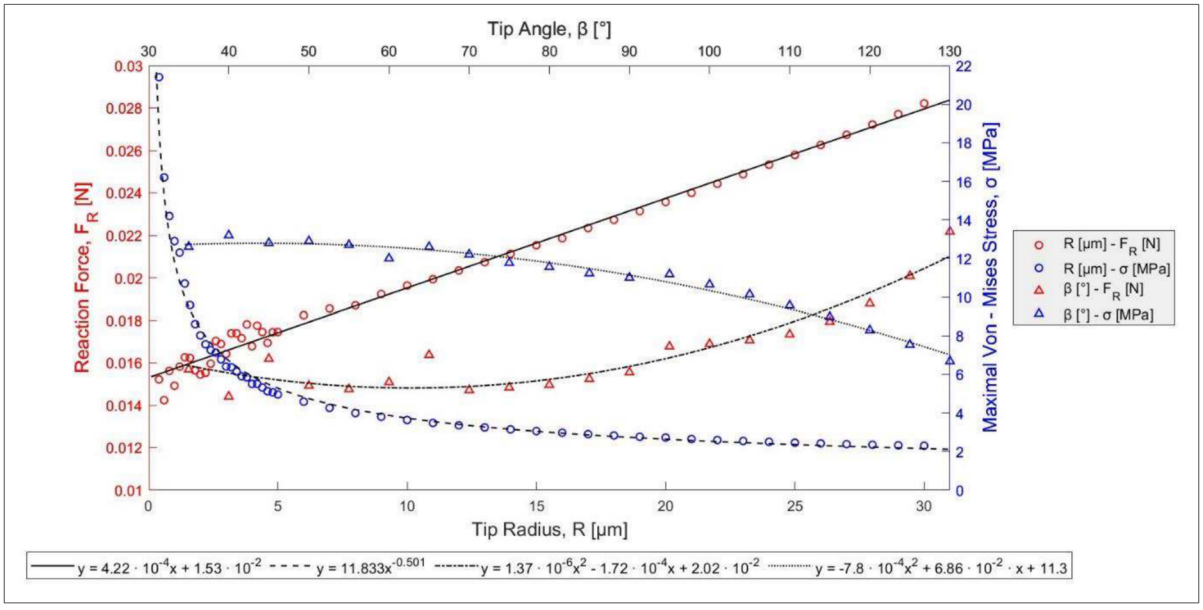

Fig. 12 FEM systematic analysis of the influence of blade's micro-geometries

polynomial order while maximal Von Mises stress decreases in similar manner. Each of these trends is in the figure represented by corresponding line and equation.

It is clear that the reaction force as well as maximal Von Mises stress are highly dependent on the blade's micro-geometry therefore it can be assumed the practical measurement of intrinsic cutting energy S_0 would follow similar dependence. Thus, noticeably if the measurement is conducted using different blade type even with the same declared thickness it must be evaluated through reference material with known T_0 to obtain appropriate parameter b (Eq. 4) which will reflect the influence of blade's micro-geometries. As was described in Fig. 7C and Fig. 9C, where effect of blade's repetition is shown, these changes to micro-

geometry as tiny and trivial as they may seem have actually significant impact on to the precision and reliability of the measurement.

4 Conclusion

In this study, several sets of boundary conditions were analysed to obtain a clear overview of their influence on Coesfeld Intrinsic Strength Analyzer (ISA) measuring methodology with final goal of improving and increasing precision and reliability of the measurement. The chosen conditions consisted of number of applied measuring strains, duration of relaxation time, specimen milling direction, blade's repetition and blades' geometry. Using reference EPDM material with known T_0 value the following findings were obtained through measured intrinsic cutting energy, S_0:

- There is no significant influence of number of applied measuring strains on S_0. This suggests that the testing protocol can be shortened by using lower number of measuring strains, thus decreasing overall duration of the analysis.
- There is no significant influence of applied relaxation time for the used reference EPDM material. However, it was noted that different behaviour might apply for different rubber types, particularly for higher Tg materials.
- For uncoated blade, there is a linear increase in S_0 with each additional blade re-use. It was noted that this phenomenon is due to the dulling mechanism which deforms the very tip of the blade. Therefore, a virgin uncoated blade must be used for each measurement.
- Polymer chains' orientation plays a significant part in the measuring procedure thus consistency in the sample orientation is highly advised.
- For coated blades, stable S_0 values are achieved regardless of the number of times the same razor blade spot is used. For the two surface treatments analysed, ceramic and TiN, it was found that the ceramic surface treatment provides completely identical S_0 values to to the first S_0 value measured on the uncoated razor blade. The TiN surface treatment increases the S_0 value significantly.
- There is a clear influence of blade's micro-geometries on resulting S_0. It was noted that value of tip radius plays prime in the cutting mechanism, followed by value of tip angle. Blades' overall thickness showed no influence. Evaluation of parameter b through reference material with known value of T_0 is highly advised when different blade type is used for the measurement.
- The overall resulting trends established blade's micro-geometry as the most influential condition followed by uncoated blade's repetition and polymer chains' orientation.

This extensive study therefore presents the sensitivity of the Lake-Yeoh cutting test parameter for measuring the intrinsic strength of rubber, thus refining the analysis of this very important parameter that can only be effectively determined by this method. By applying the results of this study, it aims to reduce standard deviations of the intrinsic strength and unify the test method across the scientific community and industry that uses this method. Considering that the study was conducted only on single rubber material, preliminary recommendations and definitions of appropriate boundary conditions will be issued after extending this study in a soon future about analyses of varied rubber and polymeric materials. Additionally, by extending this study to include an analysis of the effect of a wider range of individual applied boundary conditions, the intrinsic strength analysis method can be further refined.

Acknowledgements This project is co-financed from the state budget by the Technology Agency of the Czech Republic under the M-ERA.NET 3 Call 2021 Programme (TH80020008) within the European Union's Horizon 2020 research an innovation program under grant agreement (No. 958174)" and **by the Ministry of Education, Youth and Sports of the Czech Republic—DKRVO (RP_CPS_2024_28_006). The authors are also grateful for the funding of the grant received from The Internal Grant Agency (IGA) of TBU in Zlin—(IGA/CPS/2025/005)**

Author contributions NR: Analyses, Modelling, Simulation, Wrote the manuscriot text; RS: Design of the experiment, Analyses, Supervision, JP: Analyses; WVM: Editing, Review; TGE: Editing, Review. All authors reviewed the manuscript.

Funding Open access publishing supported by the institutions participating in the CzechELib Transformative Agreement.

Data availability The datasets generated and/or analysed during the current study are available from the corresponding author on reasonable request.

Declarations

Competing interests The authors declare no competing interests.

References

Bhowmick AK, Neogi C, Basu SP (1990) Threshold tear strength of carbon black filled rubber Vulcanizates. J Appl Polym Sci 41:917–928. https://doi.org/10.1002/app.1990.070410504

Eberlein, R., Fukada, Y., Pasieka, L. (2020). Fatigue Life Analysis of Solid Elastomer-Like Polyurethanes. In: Heinrich, G., Kipscholl, R., Stoček, R. (eds) Fatigue Crack Growth in Rubber Materials. Advances in Polymer Science, vol 286. Springer, Cham. https://doi.org/10.1007/12_2020_68

Gent AN, Tobias RH (1982) Threshold tear strength of elastomers. J Polym Sci Polym Phys Ed 20:2051–2058. https://doi.org/10.1002/pol.1982.180201107

Ghosh P, Stocek R, Gehde M, Mukhopadhyay R, Krishnakumar R (2014) Investigation of fatigue crack growth characteristics of NR/BR blend based tyre tread compounds. Int J Fract 188(1):9–21. https://doi.org/10.1007/s10704-014-9941-9

Isitman N, Stoček R, Robertson CG (2020) Influences of compounding attributes on intrinsic strength and tearing behaviour of model tread rubber compounds. In: Paper scheduled to be presented at the 197th technical meeting of the rubber division, ACS, Independence, OH, April 28–30, 2020 (Presentation slides made available online due to meeting cancellation for COVID-19 precaution)

Jin, G. Z.; Chen, L. H.; Gong, Y. Z.; Li, P.; Wang, R. G.; Li, F. Z.; Lu, Y. L. (2025) Impact of hard segment structures on fatigue threshold of casting polyurethane using cutting method. Chinese J. Polym. Sci. https://doi.org/10.1007/s10118-025-3250-9

Lake GJ, Lindley PB (1965) The mechanical fatigue limit for rubber. J Appl Polym Sci 9(4):1233–1251. https://doi.org/10.1002/app.1965.070090405

Lake GJ, Yeoh OH (1978) Measurement of rubber cutting resistance in the absence of friction. Int J Fract 14:509–526. https://doi.org/10.1007/BF01390472

Lake GJ, Yeoh OH (1987) Effect of crack tip sharpness on the strength of vulcanized rubbers. J Polym Sci, Part B: Polym Phys 25(6):1157–1190. https://doi.org/10.1002/polb.1987.090250601

Legorju-Jago K, Bathias C (2002) Fatigue initiation and propagation in natural and synthetic rubbers. Int J Fatigue 24:85–92. https://doi.org/10.1016/S0142-1123(01)00062-7

Li F, Liu J, Yang H, Lu Y, Zhang L (2016) Numerical simulation and experimental verification of heat build-up for rubber compounds. Polymer. https://doi.org/10.1016/j.polymer.2016.08.065

Mars, W. V., Robertson, C. G., Stocek, R., & Kipscholl, C. (2019) Why cutting strength is an indicator of fatigue threshold. In Constitutive models for rubber XI (pp. 351–356). CRC Press.

Mars, W. V, Sharp, E., Slovensky, J., & Stocek, R. (2022) Effect of Specimen Thickness and Blade Sharpness on Intrinsic Strength Measurements, conference proceeding, 202nd Fall Technical Meeting of the Rubber Division, American Chemical Society 2022, Held 11–13 October 2022, Knoxville, Tennessee, USA, 262–270. https://doi.org/10.52202/067657-0015

Mazich KA, Samus MA, Smith CA, Rossi G (1991) Threshold fracture of lightly crosslinked networks. Macromolecules 24:2766–2769. https://doi.org/10.1021/ma00010a020

McCarthy CT, Hussey G (2007) On the sharpness of straight edge blades in cutting soft solids: Part I–indentation experiments. Eng Fract Mech 74(14):2205–2224. https://doi.org/10.1016/j.engfracmech.2006.10.015

McCarthy CT, Ní Annaidh A (2010) On the sharpness of straight edge blades in cutting soft solids: part II–analysis of blade geometry. Eng Fract Mech 77(3):437–451. https://doi.org/10.1016/j.engfracmech.2009.10.003

Mostafa A, Abouel-Kasem A, Bayoumi MR, El-Sebaie MG (2009) On the influence of CB loading on the creep and relaxation behavior of SBR and NBR rubber vulcanizates. Mater des 30(7):2721–2725. https://doi.org/10.1016/j.matdes.2008.09.045

Peter O, Stěnička M, Heinrich G et al (2024) The tearing energy threshold of crack growth in rubber exposed to ozone: an experimental–numerical approach. Int J Fract. https://doi.org/10.1007/s10704-024-00799-y

Robertson CG, Stoček R, Stoček S, Kipscholl C, Mars W (2019) Characterizing the intrinsic strength (fatigue threshold) of natural rubber/butadiene rubber blends. Tire Sci Technol. https://doi.org/10.2346/tire.19.170168

Robertson, C.G., Goossens, J.R., Mars, W.V. (2019) Using the laboratory cutting method for predicting long-term durability of elastomers. In: Paper D15, presented at the fall 196th technical meeting of the rubber division, ACS, Cleveland, OH.

Robertson, C. G., Stoček, R., & Mars, W. V. (2021). The Fatigue Threshold of Rubber and Its Characterization Using the Cutting Method. In Advances in Polymer Science (Vol. 286, pp. 57–83). Springer Science and Business Media Deutschland GmbH. https://doi.org/10.1007/12_2020_71

Stoček, R. (2021) Some Revisions of Fatigue Crack Growth Characteristics of Rubber. In Advances in Polymer Science (Vol. 286, pp. 1–18). Springer Science and Business Media Deutschland GmbH. https://doi.org/10.1007/12_2020_72

Stoček, R., Heinrich, G., Gehde, M., Kipscholl, R. (2013). Analysis of Dynamic Crack Propagation in Elastomers by Simultaneous Tensile- and Pure-Shear-Mode Testing. In: Grellmann, W., Heinrich, G., Kaliske, M., Klüppel, M., Schneider, K., Vilgis, T. (eds) Fracture Mechanics and Statistical Mechanics of Reinforced Elastomeric Blends. Lecture Notes in Applied and Computational Mechanics, vol 70. Springer, Berlin, Heidelberg. https://doi.org/10.1007/978-3-642-37910-9_7

Stoček R, Kratina O, Kipscholl R (2015) A new experimental approach to rubber resistance against cutting by sharp objects. In: Maralova B, Petrikova I (eds) Constitutive models for rubber IX: Proceedings of the 9th European conference on constitutive models for rubbers (ECCMR IX), Prague, 1–4 Sept 2015. Balkema, Leiden, pp 357–362. https://doi.org/10.1201/b18701-65

Stoček, R., Horst, T., & Reincke, K. (2017) Tearing energy as fracture mechanical quantity for elastomers. In Advances in Polymer Science (Vol. 275, pp. 361–398). Springer New York LLC. https://doi.org/10.1007/12_2016_10

Stoček, R., Stěnička, M., Maloch, J. (2020). Determining Parametrical Functions Defining the Deformations of a Plane Strain Tensile Rubber Sample. In: Heinrich, G., Kipscholl, R., Stoček, R. (eds) Fatigue Crack Growth in Rubber Materials. Advances in Polymer Science, vol 286. Springer, Cham. https://doi.org/10.1007/12_2020_78

Tobolsky AV, Prettyman IB, Dillon JH (1944) Stress relaxation of natural and synthetic rubber stocks. Rubber Chem Technol 17(3):551–575. https://doi.org/10.5254/1.3546676

Zhang E, Bai R, Morelle XP, Suo Z (2018) Fatigue fracture of nearly elastic hydrogels. Soft Matter 14:3563–3571. https://doi.org/10.1039/C8SM00460A